






Study of Self-Homodyne Coherent System Using Multicore Fiber for Data Center Links

Xiaojun Liang , John D. Downie , *Member, IEEE*, Jason E. Hurley , Hui Su, Douglas Butler , Stephen Johnson, and William Hurley 

Abstract—The demand for information capacity in data center networks has grown exponentially during past decades. Such growth promotes consideration for adoption of coherent transmission technologies in this application space to achieve current and future high data rate requirements at 400G, 800G, and higher. Coherent systems offer higher capacity than direct detection systems using more degrees of freedom to carry information, but with higher system complexity. To meet the cost and power consumption requirements for data center transceivers, coherent-lite technologies have been proposed. Among them, self-homodyne coherent (SHC) is a promising candidate which allows the use of low cost lasers and simplifies digital signal processing (DSP). We study SHC systems and focus on the use of a multicore fiber (MCF) to obtain small channel skew, which allows for further simplification of DSP. We observe and manage stimulated Brillouin scattering (SBS) effects in the local oscillator path. We analyze the optimal power split ratio between the data path and the local oscillator path to maximize data capacity. Moreover, we compare the channel skew and transmission performance between multicore fiber and ribbon fiber. SHC with MCF delivers high data capacity with significant complexity reduction, which may be a promising solution for data center links.

Index Terms—Coherent detection, data center, multicore fiber, optical fiber communication, self-homodyne.

I. INTRODUCTION

DATA communication capacity in data center networks continues to grow exponentially. While intensity modulation direct detection (IM/DD) technologies are generally cost-effective solutions, it has become very challenging to meet the high-capacity requirements (eg. 400G, 800G and higher) at relatively long distances. Coherent communication technologies have migrated into the data center networks with link lengths on the order of tens of km. Conventional coherent communication technologies have been typically designed to maximize data capacity in long-haul and metro networks, which have high complexity and power consumption. For data center applications, it

is highly desirable to reduce complexity, power consumption and cost of coherent solutions. Since data center links are typically much shorter than long-haul and metro links, it is possible to reduce/remove some of the functionalities in conventional coherent solutions for data center applications.

Recently, simplified coherent solutions have been proposed for data center networks, including coherent-lite [1], [2], DSP-free [3], [4], and self-homodyne solutions [5]–[13]. Among these simplified solutions, self-homodyne coherent (SHC) splits the power of one laser into a data path for signal modulation and a local oscillator (LO) path where a CW laser propagates to the receiver. This allows the use of low-cost DFB lasers with \sim MHz linewidths and potentially simplifies the coherent receiver digital signal processing (DSP). Real-time SHC transmission at 600G and 800G data rates have been demonstrated recently [5], [6], [9]. SHC systems employing MCFs have been studied in [8], [9]. Also, there was a recent demonstration of an 800G LR solution using SHC to simplify DSP and to remove wavelength locking between the transmitter laser and local oscillator, which requires complex monitoring and management of laser frequencies in data center mesh networks using conventional coherent technologies [13].

In this paper, we study SHC systems and use MCF to obtain small channel skew. We evaluate experimentally the transmission performance of 80 Gbaud dual polarization 16-ary quadrature amplitude modulation (DP-16QAM) signals over a 14.3 km 4-core MCF. We observe stimulated Brillouin scattering (SBS) effects in the local oscillator (LO) path, since a high-power continuous wave (CW) laser is sent through one fiber core to act as the local oscillator at the receiver. The SBS effect limits the amount of laser power that should be launched into the LO path, which affects the optimal power splitting ratio between the data path and the LO path. We also study the impact of crosstalk from adjacent fiber cores. Transmission results show that once the signal and LO path lengths are matched in back-to-back configuration, adding the MCF does not introduce significant penalty with reduced complexity DSP. The small skews among different cores of the MCF enable successful signal constellation recovery even without carrier phase recovery, which further simplifies SHC receiver DSP. Moreover, we compare the channel skew and transmission performance between the MCF and a 12-fiber ribbon cable. We present the experimental results and analysis in Section II. The comparison with ribbon fiber is given in Section III, and in section IV we draw conclusions.

Manuscript received April 5, 2022; revised May 9, 2022; accepted May 30, 2022. Date of publication June 3, 2022; date of current version June 14, 2022. (Corresponding author: John D. Downie.)

Xiaojun Liang, John D. Downie, Jason E. Hurley, Hui Su, Douglas Butler, and Stephen Johnson are with the Corning Research and Development Corporation, Sullivan Park, Corning, NY 14870 USA (e-mail: liangx3@corning.com; downiejd@corning.com; hurleyje@corning.com; suh@corning.com; butlerdl@corning.com; johnsons2@corning.com).

William Hurley is with the Corning Optical Communications, Hickory, NC 28602 USA (e-mail: wchurley@corning.com).

Digital Object Identifier 10.1109/JPHOT.2022.3179949

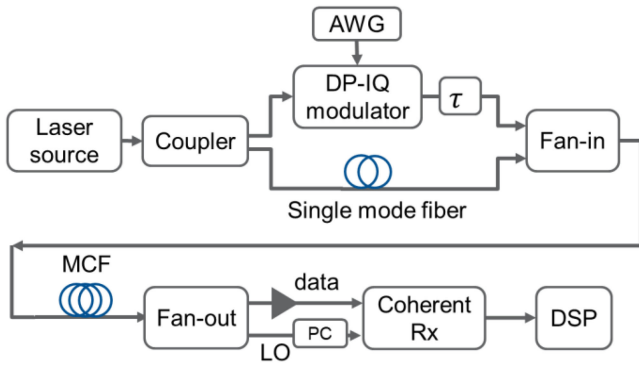


Fig. 1. Experimental setup. AWG: arbitrary waveform generator, MCF: multi-core fiber, DSP: digital signal processing, PC: polarization controller. The block τ indicates an optical delay line.

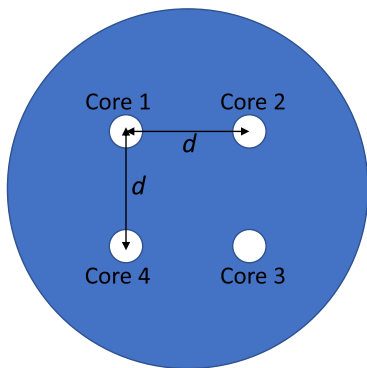


Fig. 2. Schematic diagram of the 4-core MCF. The distance d between cores was about $42 \mu\text{m}$.

II. EXPERIMENTAL SETUP AND TRANSMISSION RESULTS

A. Experimental Setup

A schematic of the experimental configuration is shown in Fig. 1. A laser source is split into two paths by a coupler. Two DFB lasers were used in experiments, with 480 kHz Lorentzian linewidth (DFB-A) and 2.2 MHz Lorentzian linewidth (DFB-B). The data path uses a dual polarization I-Q modulator to generate 80 Gbaud DP-16QAM signals. A short single-mode fiber in the LO path and an optical delay line in the signal path were added to enable matching the two path lengths in back-to-back configuration. The data signal and the CW laser are coupled into two cores of a square 2×2 four-core MCF using a fan-in. A schematic diagram of the MCF is shown in Fig. 2. The core spacing was about $42 \mu\text{m}$ and the core mode field diameters were about $9.5 \mu\text{m}$ at 1550 nm. At the output, the data signal is amplified as the laboratory coherent receiver employed for these experiments requires a minimum of 0 dBm input signal power. This amplifier may not be necessary with receivers having much better low signal power detection capability than our lab receiver. The 14.3 km MCF with fan-in/fan-outs has 3.7 dB to 4.5 dB loss depending on the core selection, as shown in Table I. In the table, note that the diagonal gray cells represent the transmission loss values at 1550 nm, while the off-diagonal cells represent the measured crosstalk values for light launched into one core

TABLE I
ATTENUATION AND CROSSTALK OF MCF WITH FAN-IN AND FAN-OUTS
(UNIT: dB)

	Core 1	Core 2	Core 3	Core 4
Core 1	-4.5	-46.5	-58.9	-46.8
Core 2	-48.6	-3.7	-47.8	-60.1
Core 3	-60.8	-47.5	-3.7	-47.9
Core 4	-47.9	-57.7	-47.3	-4.1

and detected in another. The fan-in/fan-out devices had a range of losses of about 0.4–0.8 dB. The crosstalk values between adjacent cores including the fan-in/fan-out devices were about -47 to -48 dB, and about -58 to -61 dB for diagonal cores.

The skew values of the 4-core MCF plus fan-in/fan-out devices were measured with the MCF on a large diameter (375 mm) fiber measurement spool to approximate straight deployment conditions as much as possible, and vary between 13.5 ps/km to 120.7 ps/km. The skews of the MCF alone were measured several times with both time-domain and frequency-domain approaches [14] which were found to agree very well and were stable over time. The skews of the MCF plus fan-in/fan-out devices were measured in the time-domain. We found that the fan-in/fan-out devices were well-matched in path lengths and had relatively small effects on the total skew. The smallest skew values of about 13.5 ps/km and 39 ps/km appeared to correspond to the two pairs of diagonal cores.

For the transmission experiments, received waveforms were processed offline using pilot-assisted DSP algorithms with 3% overhead of training symbols and algorithms similar to those in [15]. The DSP algorithms include dispersion compensation, clock recovery, and 2-stage polarization demultiplexing using CMA and LMS algorithms for pre-convergence and optimization, respectively, while carrier frequency offset (CFO) and carrier phase estimation (CPE) were eliminated as the same laser source is used in the SHC system. Signal to noise ratio (SNR) was evaluated based on the recovered signal constellations.

The polarization status of the CW laser may vary as it propagates along the optical fiber. This could lead to polarization fading at the coherent receiver. A few methods have been proposed to tackle this problem, by polarization tracking and compensation [5] or employing a polarization-maintaining channel [9]. In a lab environment, we observed that the polarization status of the CW laser changes very slowly. We obtained sufficiently stable results by manually tuning using a polarization controller located in the LO path directly before the coherent receiver and subsequently capturing waveform sequences.

To begin, we aligned the lengths of the data path and the LO path in the back-to-back (B2B) configuration, without the MCF or fan-in/fan-out devices. A CW laser was modulated with a pulse sequence of ~ 1 GHz repetition frequency and then launched into the coupler before splitting into two paths. We used a real-time oscilloscope to measure the signal detected by the coherent receiver. When the two path lengths are matched, the optical pulses will beat with each other and generate an electrical signal in the oscilloscope. By varying the length of

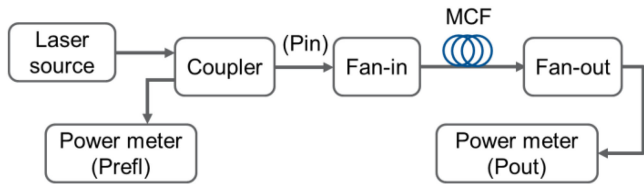


Fig. 3. Experimental setup for measuring SBS effects. P_{in} : input power, MCF: multicore fiber, P_{refl} : reflected power, P_{out} : output power.

the single mode fiber (SMF) and the optical delay line, the two path lengths can be matched by maximizing the amplitude and achieving equal electrical pulse width on the oscilloscope as the original pulse. As the pulse sequence is repetitive, we repeated the measurements by varying the sequence repetition frequency to avoid the case when the pulses from the two paths are off by a multiple of repetition periods. After the alignment, the B2B received signal measurement showed 16.1 dB SNR. It is worth mentioning that the B2B path alignment is necessary in our laboratory experiments where discrete components are used. In a real system with integrated transceivers, the form factor is much smaller. The lengths of both paths in B2B would be small and path differences may be negligible, assuming fan-in/fan-out device paths can also be well-matched.

B. Impact of Stimulated Brillouin Scattering Effects

In a SHC system, the same laser output power is split into two paths to modulate the data signal and to act as a local oscillator at the receiver. The optimal power split ratio has previously been shown to be an even 50:50 allocation to the two paths [16]. A simple explanation is as follows. Consider a laser with total power P_{tot} . The power split into the two paths is P_1 and P_2 . $P_{tot} = P_1 + P_2$ for simplicity. Assume the link losses of the two paths to be A_1, A_2 , which are independent of the power splitting ratio. Then the output electrical signal from a coherent receiver is proportional to $\sqrt{A_1 A_2 P_1 P_2}$. To optimize system SNR, one needs to maximize $\sqrt{A_1 A_2 P_1 P_2}$. Given $P_{tot} = P_1 + P_2$, the optimal condition is $P_1 = P_2 = P_{tot}/2$, indicating 50:50 to be the optimal power splitting ratio. However, we note that this simple analysis does not account for other effects in SHC systems including OSNR which are directly related to power split ratio [17].

In addition to OSNR, the analysis in the above paragraph ignores the dependence of other effects on input power levels. We observed in experiments that SBS effects can occur when a high-power CW laser is launched into the fiber core of the LO path. We measured the reflected and transmitted power through the MCF using a setup shown in Fig. 3. The reflected power for both lasers, and normalized loss for DFB-A are shown in Fig. 4 as a function of input power. It clearly shows that reflected power increases significantly when the input power exceeds ~ 8 -10 dBm, indicating SBS effects. In transmission experiments, the SBS effects lead to two penalties: (i) the fiber link loss (A_1) increases as the CW laser power exceeds the threshold, (ii) the reflected optical power interferes with the signal power and leads to waveform fluctuations with time. To

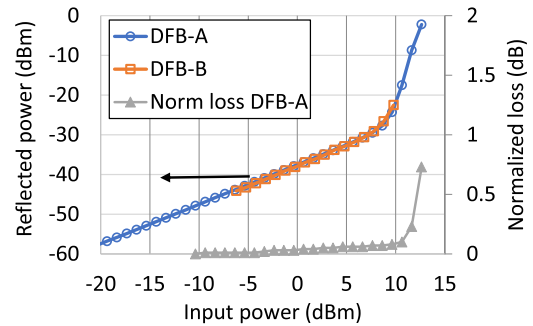


Fig. 4. Measured CW power reflected from MCF and normalized loss through MCF under different input laser power levels.

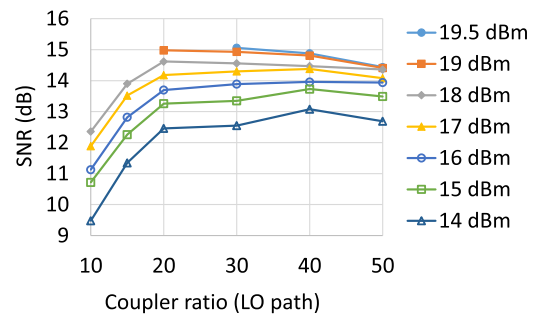


Fig. 5. SNR of systems with different coupler ratios and laser powers. The horizontal axis represents the power percentage that launches into the local oscillator path.

minimize the penalty due to SBS effects, the power split ratio would allocate no more than the SBS threshold (~ 8 dBm) into the LO path, while allocating all the remaining power into the data path. We note that this threshold is that of the combined fan-in device plus MCF, which includes the fan-in loss. This helps to improve the optical signal to noise ratio (OSNR) of the received signal, as there is substantial insertion loss (~ 27 dB) of the modulator in the data path.

The 4-core MCF deployed on the 375 mm diameter spool was then added to the link including the fan-in and fan-out devices. We measured the transmission performance of systems with different coupler ratios and laser power levels of DFB-A. Fig. 5 shows the measured SNR as a function of the LO path coupler ratio. For lower laser power levels, the SNR is relatively flat for ratios of 20-50%, while for higher laser powers, the SNR appears to slowly decline over that range which may be due to SBS effects. For these measurements, we chose core 2 and 4 for the LO and data paths respectively, as will be explained in the next Section. Also, phase noise compensation was turned on in DSP to avoid any differences that may arise due to the length variations in the coupler pigtailed, since our focus is to study the impact of power allocation. As the laser power increases, the optimal coupler ratio changes to direct less power in the LO path which mitigates SBS effects. In the experiments, the laboratory transmitter module has a maximum specified input power of 16 dBm given by the manufacturer, so that we could not test very small coupler ratios for the highest laser powers.

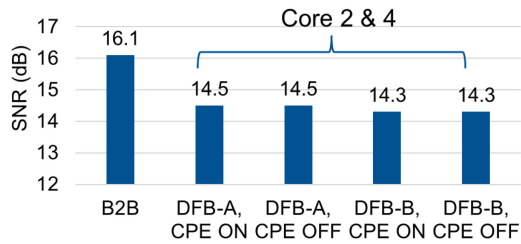


Fig. 6. SNR comparisons with CPE on and off.

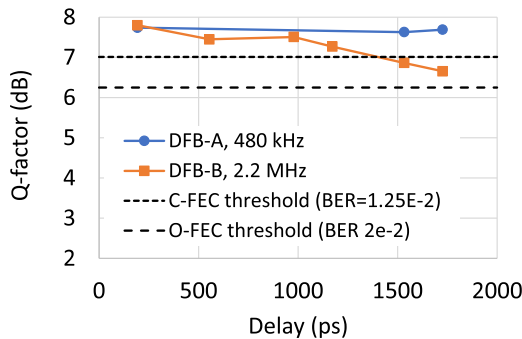


Fig. 7. Q-factor of the six possible core pairs of the 2×2 MCF.

In the following transmission experiments, the maximum power of DFB-B is 17.6 dBm. For fair comparison, we chose to use 17.6 dBm for both DFB-A and DFB-B in experiments. The corresponding power split ratio used was 30:70 for the relative powers directed to the local oscillator and signal paths, respectively.

C. Skew Tolerance

To assess the impact of MCF core-to-core skew on transmission performance, we started using core 2 and core 4 for the LO and data paths respectively, since these cores had the smallest relative skew of 13.5 ps/km. Given the small skew, it was not necessary to re-adjust the path length alignment. Transmission experiments were conducted using DFB-A and DFB-B, and with CPE turned ON and OFF. Fig. 6 shows that the 14.3 km MCF introduces a small SNR penalty of 1.6 dB to 1.8 dB. We attribute the difference in SNR between B2B and transmission through the MCF with CPE turned ON to lower OSNR and lower LO received power during transmission, as well as a small contribution from SBS. The lower received power during transmission also required changes in the physical RF channels in the real-time oscilloscopes sampling the signal and resulted in higher receiver noise. Turning off the CPE and CFO in DSP did not produce any SNR penalty for this pair of cores in the MCF. The total skew for this core pair over the 14.3 km length was about 15 symbol periods. These results may be largely consistent with previous work that has addressed the impact of skew on signal performance [18], [19].

We next studied transmission performance using different core pairs of the 4-core MCF. Fig. 7 shows the Q-factor as a function of total accumulated delay over the 14.3 km length. The six measurements correspond to the six different core pairs.

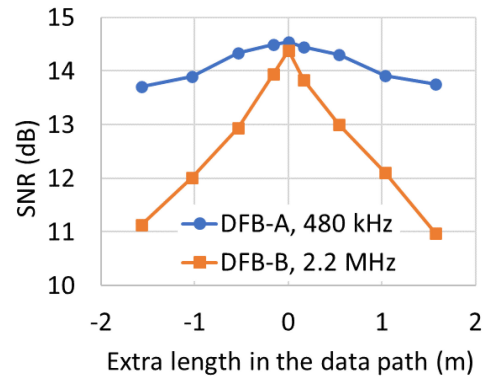


Fig. 8. Skew tolerance. SNR as a function of extra fiber length added to the data path.

TABLE II
IMPACT OF MCF CROSSTALK (SIGNAL WAVELENGTH AT 1556.56 nm)

	Without crosstalk channels	One side LO crosstalk term at 1556.56 nm	Two LO crosstalk terms at 1556.56 nm	Two LO crosstalk terms at 1556.18 nm
SNR (dB)	14.4	14.0	13.8	14.3

Using the 480 kHz DFB-A, the received SNR varies negligibly among different core pairs. Using the 2.2 MHz DFB-B, the Q-factor varies by about 1 dB over the different core pairs. The Q-factor thresholds are also shown for 400G-ZR C-FEC (BER = $1.25e-2$, $Q^2 = 7.01$ dB) and 400G-ZR+ O-FEC (BER = $2e-2$, $Q^2 = 6.25$ dB). All core pairs pass for O-FEC, while 4 out of 6 core pairs pass for C-FEC. Assuming 17% total overhead, the achieved data rate is 531 Gb/s. These experimental results indicate that all six core pairs of this MCF support SHC transmission without additional path length alignment or CPE in DSP, at least for the higher BER threshold of O-FEC. MCF with higher inter-core skews may only support shorter link lengths [20]–[22].

We further investigated the tolerance of length mismatch by adding extra fiber lengths to the signal path or the LO path when cores 2 and 4 were used in the MCF. Fig. 8 shows that SNR decreases as the SHC system deviates from the path matching condition. At 1-dB SNR penalty, the length mismatch is ~ 2.0 m for DFB-A and 0.3 m for DFB-B.

D. Impact of Crosstalk

SHC with 4-core MCF can be used as a bi-directional link, with 2 cores for each direction. Our experiments only used 2 cores, while there was no optical power in the remaining cores. In order to briefly study the impact of crosstalk, we measured transmission performance and transmitted additional LO power (which is much stronger than the signal) in the same direction as worst-case crosstalk in the remaining cores, as shown in Table II. The signal and normal LO lightwaves were launched in cores 2 and 4 with DFB-B. When we launched another laser (a tunable external cavity laser) with the same wavelength and the same power as the LO path in the co-propagating direction in a third core, we observed an SNR penalty due to crosstalk of approximately 0.4 dB. For two extra LO signals launched in the

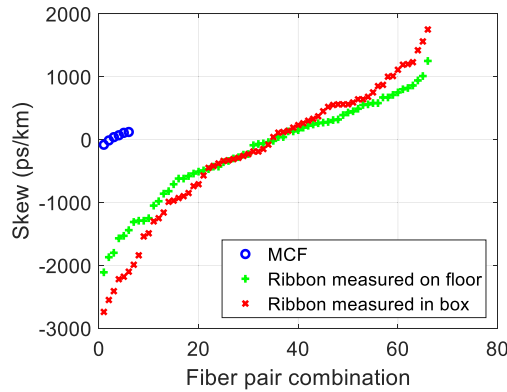


Fig. 9. Skew comparison between MCF and ribbon fiber.

third and fourth cores (beyond a realistic situation), the penalty was about 0.6 dB. In real systems, the interfering LO power would likely be counter-propagating in the opposite direction and could also have a slightly different wavelength. Each of those conditions would lead to a significantly lower crosstalk penalty. We measured the crosstalk penalty to be less than 0.1 dB when the wavelength is tuned off by about 50 GHz in the co-propagation configuration. Note that with lower quality and uncooled DFB lasers wavelength stability may be variable so the case measured with a same wavelength co-propagating crosstalk laser may be the worst case and relatively infrequent.

III. COMPARISON WITH RIBBON FIBER

An alternative solution is to use separate single mode fibers instead of MCF in SHC systems. To assess this approach, we measured the skew in a typical 12-fiber ribbon cable [23]. Fig. 9 compares the skew of our 4-core MCF and a 12-fiber ribbon cable. The ribbon fiber was measured under two conditions: (i) coiled in a shipping box, (ii) uncoiled onto the floor. It is difficult to know exactly why the range of skews are somewhat different for the ribbon in the two conditions, but the data illustrates the ranges for a particular cable under two conditions. There are 6 possible skew values for the 2×2 MCF and 66 possible skew values for the 12-fiber ribbon. The MCF has more than an order of magnitude lower skew than the ribbon fiber. It is worth mentioning that the MCF was not specifically designed for low skew, and it is possible to optimize MCF designs to minimize skew through careful matching of core properties [23] and fiber twist [24].

Fig. 10 compares the transmission performance of the 14.3 km length of MCF and a 12.5 km length of typical ribbon fiber. The path lengths were aligned in B2B configuration and not adjusted after including the fiber links. The CPE in DSP was turned off. For the MCF, all six possible fiber pairs were measured. For the ribbon fiber, two fibers on each end and two fibers in the middle were measured in various pairings, with fiber IDs [1], [2], [6], [7], [11], [12]. Fig. 10 shows that the SNR varies in a much smaller range in MCF than in the ribbon fiber. To use separate fibers for SHC transmission, it might be necessary to re-adjust the path alignment manually with the specific fiber pair or to use CPE in DSP.

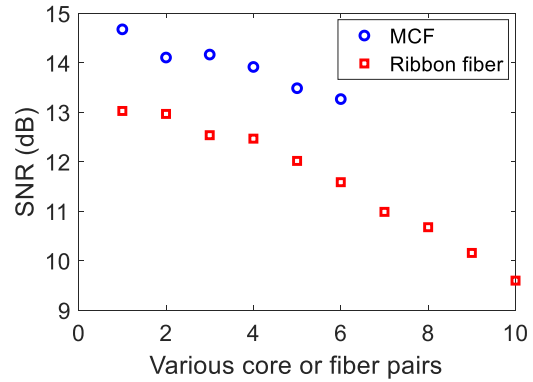


Fig. 10. SNR comparison between MCF and ribbon fiber.

IV. CONCLUSION

We have studied a self-homodyne coherent system using multicore fibers for data center links. We measured the transmission of 80 Gbaud DP-16QAM signals over a 14.3 km 4-core MCF. We observed SBS effects while transmitting a CW laser in the local oscillator path and analyzed its impact on the optimal power splitting ratio between the two paths. We studied the impact of crosstalk in different pairs of MCF channels. We also compared the skew and transmission performance of MCF with ribbon fibers. The experimental results show that self-homodyne coherent systems using MCF may be a promising solution for data center networks and may allow the use of low-cost DFB lasers and low-complexity DSP. We note that while the results presented here were for a 16QAM format, higher modulation formats such as 64QAM and above are theoretically less tolerant to phase noise and crosstalk and thus may require smaller skews to enable DSP complexity reduction.

REFERENCES

- [1] O. Ishida, K. Takei, and E. Yamazaki, "Power efficient DSP implementation for 100G-and-beyond multi-haul coherent fiber-optic communications," in *Proc. Opt. Fiber Commun. Conf. Exhib.*, 2016, pp. 1–3.
- [2] T. Kupfer, A. Bisplinghof, T. Duthel, C. Fludger, and S. Langenbach, "Optimizing power consumption of a coherent DSP for metro and data center interconnects," in *Proc. Opt. Fiber Commun. Conf. Exhib.*, 2017, pp. 1–3.
- [3] J. K. Perin, A. Shastri, and J. M. Kahn, "Design of low-power DSP-free coherent receivers for data center links," *J. Lightw. Technol.*, vol. 35, no. 21, pp. 4650–4662, Nov. 2017.
- [4] M. Morsy-Osman *et al.*, "DSP-free 'coherent-lite' transceiver for next generation single wavelength optical intra-datacenter interconnects," *Opt. Exp.*, vol. 26, no. 7, pp. 8890–8903, 2018.
- [5] T. Gui, X. Wang, M. Tang, Y. Yu, Y. Lu, and L. Li, "Real-time demonstration of 600 Gb/s DP-64QAM self-homodyne coherent bi-direction transmission with un-cooled DFB laser," in *Proc. Opt. Fiber Commun. Conf. Exhib.*, 2020, pp. 1–3.
- [6] L. Wang *et al.*, "First real-time MIMO-free 800 Gb/s DP-64QAM demonstration using bi-directional self-homodyne coherent transceivers," in *Proc. Eur. Conf. Opt. Commun.*, 2021, Paper PD1.5.
- [7] X. Zhou, Y. Gao, J. Huo, and W. Shieh, "Theoretical analysis of phase noise induced by laser linewidth and mismatch length in self-homodyne coherent systems," *J. Lightw. Technol.*, vol. 39, no. 5, pp. 1312–1321, Mar. 2021.
- [8] M. Liu and W. Fu, "Multi-core fiber based coherent transceiver utilizing self-homodyne detection and ICA based channel equalization for optical intra-datacenter interconnects," *Optik*, vol. 205, 2020, Art. no. 164215.
- [9] T. Gui *et al.*, "Real time 6.4 TBPS (8×800 G) SHCD transmission through $1 + 8$ multicore fiber for co-packaged optical-IO switch applications," in *Proc. Opt. Fiber Commun. Conf. Exhib.*, 2022, pp. 1–3.

- [10] R. Zhang, Y. W. Chen, K. Kuzmin, and W. I. Way, "Intra-data center 120 Gbaud/DP-16QAM self-homodyne coherent links with simplified coherent DSP," in *Proc. Opt. Fiber Commun. Conf.*, 2022, pp. 1–3, Paper W1G-1.
- [11] E. Ip, Y. K. Huang, T. Wang, Y. Aono, and K. Asahi, "Distributed acoustic sensing for datacenter optical interconnects using self-homodyne coherent detection," in *Proc. Opt. Fiber Commun. Conf. Exhib.*, 2022, pp. 1–3.
- [12] Y. Gao, X. Zhou, F. Li, J. Huo, J. Yuan, and K. Long, "Mismatch length estimation of self-homodyne coherent optical systems by using carrier-pilot-assist method," in *Proc. Opt. Fiber Commun. Conf. Exhib.*, 2022, pp. 1–3.
- [13] Lightwave, "NeoPhotonics demos 120- Gbaud components," [Online]. Available: https://www.lightwaveonline.com/optical-tech/components/article/14234937/neoPhotonics-demos-120gbaud-components?utm_source=LW%20Enabling%20Tech&utm_medium=email&utm_campaign=CPS220303121&o_eid=1984G0325167J9V&rdx.ident%5Bpull%5D=omeda%7C1984G0325167J9V&oly_enc_id=1984G0325167J9V
- [14] X. Chen, K. Li, J. Hurley, and M.-J. Li, "Simultaneously measuring group delays, chromatic dispersion and skews of multicore fibers using a frequency domain method," in *Proc. Opt. Fiber Commun. Conf. Exhib.*, 2022, pp. 1–3.
- [15] Y. Wakayama, E. Sillekens, L. Galdino, D. Lavery, R. I. Killey, and P. Bayvel, "Increasing achievable information rates with pilot-based DSP in standard intradyne detection," in *Proc. 45th Eur. Conf. Opt. Commun.*, 2019, pp. 1–4, doi: [10.1049/cp.2019.0888](https://doi.org/10.1049/cp.2019.0888).
- [16] T. Gui, X. Wang, M. Tang, Y. Yu, Y. Lu, and L. Li, "Real-time demonstration of self-homodyne coherent bidirectional transmission for next-generation data center interconnects," *J. Lightw. Technol.*, vol. 39, no. 4, pp. 1231–1238, Apr. 2021.
- [17] R. S. Luís *et al.*, "OSNR penalty of self-homodyne coherent detection in spatial-division-multiplexing systems," *IEEE Photon. Technol. Lett.*, vol. 26, no. 5, pp. 477–479, Mar. 2014, doi: [10.1109/LPT.2013.2297445](https://doi.org/10.1109/LPT.2013.2297445).
- [18] J. M. D. Mendinueta *et al.*, "Investigation of receiver DSP carrier phase estimation rate for self-homodyne Space-division multiplexing communication systems," in *Proc. Opt. Fiber Commun. Conf. Expo. Nat. Fiber Optic Engineers Conf.*, 2013, pp. 1–3.
- [19] R. S. Luís, B. J. Puttnam, J. M. Delgado Mendinueta, Y. Awaji, and N. Wada, "Impact of spatial channel skew on the performance of spatial-division multiplexed self-homodyne transmission systems," in *Proc. Int. Conf. Photon. Switching*, 2015, pp. 37–39, doi: [10.1109/PS.2015.7328945](https://doi.org/10.1109/PS.2015.7328945).
- [20] R. S. Luís, B. J. Puttnam, J. -M. Delgado Mendinueta, W. Klaus, Y. Awaji, and N. Wada, "Comparing inter-core skew fluctuations in multi-core and single-core fibers," in *Proc. Conf. Lasers Electro-Opt.*, 2015, pp. 1–2, doi: [10.1364/CLEO_SI.2015.SM2L.5](https://doi.org/10.1364/CLEO_SI.2015.SM2L.5).
- [21] B. J. Puttnam, G. Rademacher, R. S. Luís, J. Sakaguchi, Y. Awaji, and N. Wada, "Inter-core skew measurements in temperature controlled multi-core fiber," in *Proc. Opt. Fiber Commun. Conf. Expo.*, 2018, pp. 1–3.
- [22] R. Luis *et al.*, "Compensation of inter-core skew in multi-core fibers with group velocity dispersion," *Opt. Exp.*, vol. 29, no. 18, pp. 28104–28109, Aug. 2021.
- [23] D. J. Hession, S. S. Sodhi, W. S. Jackman, and W. C. Hurley, "Skew testing for parallel optics systems," in *Proc. 57th Int. Wire Cable Symp.*, 2008, pp. 312–319.
- [24] Y. Sasaki, K. Hirakawa, I. Ishida, S. Matsuo, and K. Aikawa, "Evaluation of inter-core skew in an uncoupled multicore fibre," in *Proc. Eur. Conf. Opt. Commun.*, 2017, pp. 1–3.